

# 1 Introduction

Langmuir probes are the oldest type of plasma diagnostic device and are still one of the most frequently employed tools used to obtain information about conditions inside a plasma. In relation to tokamaks, Langmuir probes are the most reported edge diagnostic in the literature [1]. The main advantage of using probes is that they can make highly localised measurements, almost all other diagnostics give volume averaged measurements. Readings from Langmuir probes are an essential input into simulation codes that aim to simulate the edge region of a tokamak, as the probes measure plasma conditions at solid surfaces, which is typically the most important output from modelling codes. These codes require inputs with high spatial and temporal resolution [2]. The probes take their name from the Nobel prize winning scientist Irving Langmuir who coined the term plasma and whose paper published in 1926 with H.M. Mott-Smith provided a means to measure plasma parameters by obtaining a Current-Voltage curve (IV curve) using a probe [3]. The probe in its simplest form is a metallic electrode, electrically biased with respect to a reference electrode which is then inserted into a plasma to draw an ion or electron current. Electrical probes are used to diagnose a wide range of plasmas from space plasmas with low-density and weak magnetic fields to those at the edge of nuclear fusion devices with hostile conditions to material surfaces and strong magnetic fields. The use of probes requires direct contact to be made between the probe and the plasma and so their use is limited by the conditions in which they can survive. This restricts the use of probes to the edge of tokamak devices where the plasma is less dense and cooler.

Langmuir probes are a powerful diagnostic capable of providing local measurements of the plasma potential ( $V_p$ ), electron density ( $n_e$ ) and electron temperature ( $T_e$ ) with a good time resolution of approximately  $10^{-3}$  seconds [4]. They are fairly easy both to design and build and acquiring data from them is straightforward. Despite their simplicity in construction and operation, probes do have a downside compared to other diagnostics. As probes are in contact with the plasma, they perturb it, changing the local density and potential in the surrounding plasma. This complicates the interpretation of probe data. The role of probe theory is to determine the unperturbed values of the plasma which would exist in the absence of the probe. However theoretical models used to interpret the data can be very complicated and in

some cases non-existent. No general model exists that is capable of relating the measured current voltage curves with the actual plasma properties under all possible physical conditions. An overview of the general probe method will be given followed by complications that arise, specifically in the presence of magnetic fields.

## 2 Sheath Physics

In order to understand particle collection by a Langmuir probe it is essential to realise the role played by the plasma sheath. An electrostatic sheath forms whenever a material object comes into contact with a plasma. The sheath dominates the transport of ions and electrons to the material surface. The difference in mobility between electrons and ions is the foundation for the formation of a sheath. For example, consider the case of a divertor tile coming into contact with plasma. Before contact with the plasma, there is no net charge on the tile, the tile is neutral. As the plasma reaches the tile, electrons in the plasma will rush to the tile ahead of the ions. This occurs because electrons are much less massive than ions and so move around much faster in the plasma. This process can not go on indefinitely. A net negative charge builds up on the tile which leads to the formation of a potential barrier. This barrier repels electrons and attracts ions [5]. The potential barrier continues to increase, reducing the electron flux until a steady state is obtained once the electron flux becomes equal to the ion flux. The potential of the tile at steady state is the floating potential  $V_F$ . The tile is said to be floating. The potential a floating object reaches depends on the plasma potential, the temperature of the electrons and ions and the mass ratio of the charged particles. This will be derived in section ??.

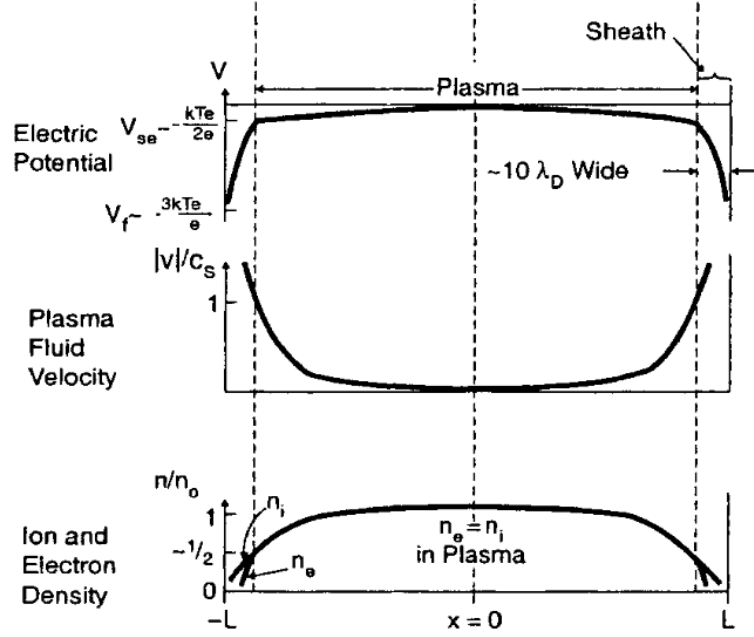


Figure 1: A schematic of the variation of electric potential, plasma velocity and particle density with distance from the wall in a plasma [6].

The floating tile is a region of charge in an otherwise quasineutral plasma. The behaviour of the plasma in response to the presence of this charge is governed by the Poisson equation

$$\nabla^2 \psi = -\frac{e}{\epsilon_0} (n_i - n_e) \quad (1)$$

where  $\psi$  is the potential at a given point in the plasma,  $e$  the electron charge,  $n_i$  the ion density, assuming singly charged ions and  $n_e$  the electron density. The electrons mobility allows them to react quickly to the charge and they adopt a Boltzmann distribution

$$n_e = n_\infty \exp\left(\frac{e\psi}{T_e}\right) \quad (2)$$

where  $n_\infty$  is the plasma density, for both electrons and ions, far from the external charge and  $T_e$  is the electron temperature. Over fast timescales the ions can be considered stationary. Substituting equation 2 into equation 1

gives

$$\nabla^2 \psi = -\frac{en_i}{\epsilon_0} \left( 1 - \exp \left( \frac{e\psi}{T_e} \right) \right) \quad (3)$$

By expanding the exponential term and assuming  $T_e \gg e\psi$  we find

$$\nabla^2 \psi \approx \frac{e^2 n_i}{\epsilon_0 T_e} \psi = \frac{\psi}{\lambda_D^2} \quad (4)$$

where  $\lambda_D$  is the Debye length. Expanding equation 4 we find

$$\psi = \psi_0 \exp \left( -\frac{x}{\lambda_D} \right) \quad (5)$$

the potential of the charge drops off exponentially with distance into the plasma. The Debye length is then the distance over which the charge can penetrate into the plasma. This thin layer where the potential from the charge is able to influence the plasma is known as the sheath. The sheath is a transition layer in the plasma between an external charge and the bulk plasma. In the sheath, quasi-neutrality no longer holds. The sheath acts to shield the rest of the plasma from the external charge. In the case of a negatively floating tile, the potential from the tile will be contained in the sheath region. Ions are accelerated in the sheath towards the tile while the electrons are de-accelerated. In order for the sheath to be stable, the ions must enter the sheath with sufficient velocity such that  $v \geq c_s$  where  $c_s$  is the plasma sound speed. This is the well known Bohm Criterion [7]. It is possible to derive this result by considering a 1D, unmagnetised plasma in contact with a material surface as shown in figure 1. In the bulk plasma the plasma potential is zero. We assume the ions are born stationary and cold, far from the tile, in the bulk plasma. It is assumed the electrons have a Maxwellian distribution so that their density profile can be described by the Boltzmann relation

$$n_e = n_{se} e^{\frac{e(V-V_{se})}{KT_e}} \quad (6)$$

where  $n_{se}$  is the electron density at the sheath entrance,  $V_{se}$  the plasma potential at the sheath entrance,  $K$  the Boltzmann constant and  $T_e$  the electron temperature in Kelvin. This is a valid approximation as most electrons are reflected in the sheath and so the Maxwellian distribution is maintained. There is a potential drop between the bulk plasma and the sheath entrance, in other words,  $V_{se}$  is negative relative to the plasma potential. This potential

drop occurs in a region of plasma known as the pre-sheath. It is this drop in potential that accelerates the ions so that they satisfy the Bohm Criterion. For the ions we apply conservation of energy which leads to

$$\frac{1}{2}m_i v^2 = -e\psi \quad (7)$$

This equation is valid at all points in the plasma. From particle conservation, in the absence of sources and sinks, we have

$$n_i v_i = n_{se} v_{se} \rightarrow n_i = \frac{n_{se} v_{se}}{v_i} \quad (8)$$

From energy conservation we have

$$v_{se} = \left(-\frac{2e\psi_{se}}{m_i}\right)^{1/2} \quad v_i = \left(-\frac{2e\psi}{m_i}\right)^{1/2} \quad (9)$$

Plugging this into equation 8 gives

$$n_i = n_{se} \left(\frac{\psi_{se}}{\psi}\right)^{1/2} \quad (10)$$

Substituting equations 10 and 6, for the ion density and electron density respectively, into Poissons equation, equation 1 and we get

$$\frac{d^2\psi}{dx^2} = -\frac{e}{\epsilon_0} n_{se} \left[ \left(\frac{\psi_{se}}{\psi}\right)^{1/2} - \exp\left[\frac{e(\psi - \psi_{se})}{kT_e}\right] \right] \quad (11)$$

This is valid in both the bulk plasma and the sheath. We now define a variable  $\Delta$  such that

$$\Delta = \psi_{se} - \psi \quad (12)$$

In the sheath region  $\psi < \psi_{se}$  therefore  $\Delta > 0$ . We can now carry out an expansion of the two terms on the right hand side of equation 11.

$$\left(\frac{\psi_{se}}{\psi}\right)^{1/2} = \left(\frac{\Delta}{\psi} + 1\right) \approx 1 + \frac{\Delta}{2\psi} = 1 - \frac{\Delta}{2|\psi_{se}|} \quad (13)$$

Here we take a point just inside the sheath such that  $\psi \approx \psi_{se}$ . The second substitution and expansion gives

$$\exp\left[\frac{e(\psi - \psi_{se})}{kT_e}\right] = \exp\left[\frac{-e\Delta}{kT_e}\right] \approx 1 - \frac{e\Delta}{kT_e} \quad (14)$$

We can now substitute equations 12,13 and 14 into equation 11.

$$\frac{d^2\Delta}{dx^2} = \frac{e}{\epsilon_0} n_{se} \left[ \frac{e\Delta}{kT_e} - \frac{\Delta}{2|\psi_{se}|} \right] \quad (15)$$

This will only provide non-oscillatory solutions when

$$\frac{e}{kT_e} \geq \frac{1}{2|\psi_{se}|} \quad (16)$$

Which, with the use of equation 9 can be recast as

$$v_{se} \geq \sqrt{\frac{kT_e}{m_i}} \quad (17)$$

which is the Bohm criterion with  $c_s = \sqrt{\frac{kT_e}{m_i}}$ . Ions are accelerated in the pre-sheath which penetrates deep into the plasma. In deriving this value for  $c_s$  it was assumed that the ions are cold. By relaxing this assumption and having ions with a finite temperature, a new value for the sound speed can be obtained [8]

$$c_s = \sqrt{\frac{k(T_e + T_i)}{m_i}} \quad (18)$$

### 3 Ideal Probe Theory

The method for obtaining probe data is relatively simple. The probe is immersed in plasma and then biased to a potential ( $V_B$ ) by an external circuit. The collected current ( $I_p$ ) is then recorded at different probe voltages allowing an IV curve to be produced. The plasma parameters are then deduced from this IV characteristic. Charged particles are drawn to the probe by the surrounding electric field which extends a few Debye lengths into the plasma, in the sheath region. The theory developed by Langmuir and Mott-Smith allows the plasma parameters to be deduced for unmagnetised plasmas with a Maxwellian distribution of ions and electrons. This theory will be discussed before moving on to fusion relevant plasma conditions.

When a probe is inserted into a plasma it is bombarded by neutral particles and the charged electrons and ions. Absent of any electric forces, the

impact rate per  $m^2$  for each species is given by their random thermal flux ( $\Gamma$ ) which can be expressed as

$$\Gamma_s = \frac{1}{4}n_s\langle v_s \rangle \quad (19)$$

where  $n_s$  is the number density of that particular species and  $\langle v_s \rangle$  the average speed. For a Maxwellian distribution of particles this can be expressed as

$$\Gamma_s = \frac{1}{4}n_s\sqrt{\frac{8kT_s}{\pi m_s}} \quad (20)$$

During probe operation, the probe voltage is swept from negative to positive while the current collected by the probe is recorded in order to produce the IV curve. Data for the entire curve is typically obtained in microseconds but this can be reduced. Advanced probe techniques are capable of completing a voltage sweep in  $\approx 10^{-8}$  s [9]. The current collected by the probe will be composed of ions or electrons or a combination of both depending on the applied potential of the probe. For  $V_B = V_F$ , no net current is drawn from the plasma as the electron flux reaching the probe is balanced by the ion flux. For  $V_B > V_F$  the electron flux exceeds the ion flux and therefore a net current will flow into the plasma while for  $V_B < V_F$  the ion flux exceeds the electron flux therefore a net current flows out of the plasma. For this report the sign convention declares current entering the plasma as a negative current and current leaving the plasma as positive current. A typical ideal IV curve is shown in figure 2. The curve is described as ideal because it is a theoretical prediction of an IV curve in an unperturbed plasma. Experimental IV curves deviate from the ideal case, as will be discussed.

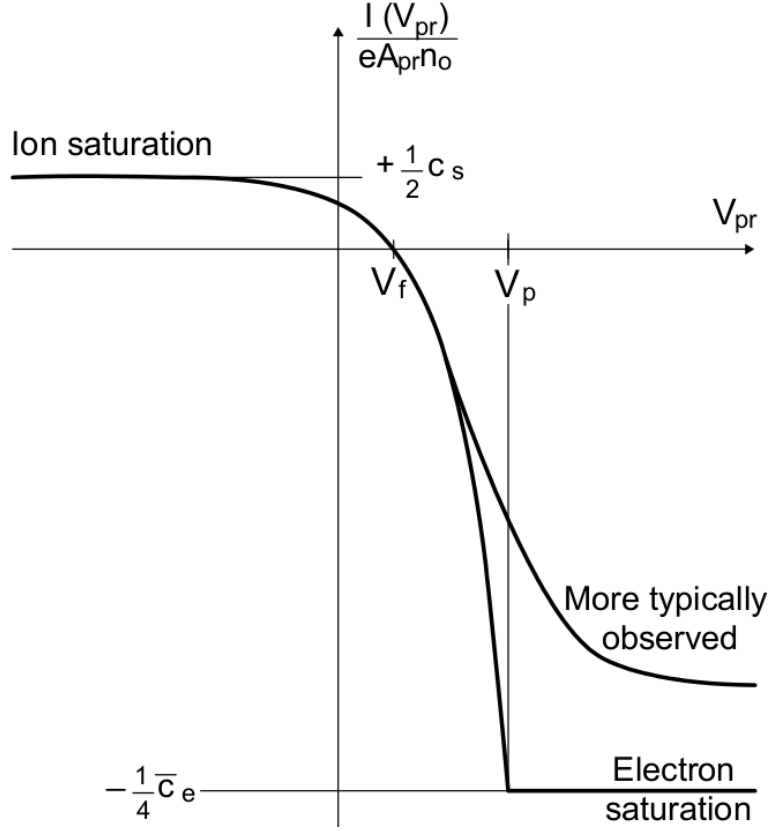


Figure 2: A schematic of the IV curve obtained with a single Langmuir probe [10].

If no bias voltage is applied to the probe, the probe is allowed to float and will quickly charge up negative until it reaches the floating potential ( $V_F$ ). At floating potential the probe collects zero net current from the plasma. The floating potential is labelled on figure 2. It is less than the plasma potential ( $V_p$ ) as a negative bias is required to retard the flow of electrons and accelerate ions in order to balance the two fluxes. While  $V_B < V_p$  the probe is biased negatively with respect to the plasma potential therefore ion collection to the probe is unhindered and so ions are collected at a saturated rate. If the probe bias is sufficiently negative all electrons are repelled and the current collected by the probe is then the ion saturation current approximated by the Bohm current

$$I_{sat}^+ = n_{i,sheath} e c_s A \quad (21)$$



where  $n_{i,sheath}$  is the ion density at the sheath edge,  $e$  is the fundamental charge and  $A$  the area of the exposed probe tip. The ion flux is independent of the applied potential so making the probe more negative will not result in an increase in probe current.

As the bias voltage increases (becomes more positive), the sheath potential drop is reduced allowing electrons at the high energy tail of the distribution to reach the probe. This region of the curve is known as the transition region. As  $V_B \rightarrow V_p$  more and more electrons are able to reach the probe as less kinetic energy is needed to overcome the potential. For a Maxwellian distribution of electrons and neglecting effects such as secondary electron emission, the electron current able to reach the probe in the transition region is given by

$$I^- = \frac{1}{4} n_0 e A \sqrt{\frac{8kT_e}{\pi m_e}} \exp \left[ \frac{e(V_B - V_p)}{kT_e} \right] \quad (22)$$

The term  $\sqrt{\frac{8kT_e}{\pi m_e}}$  will be denoted as  $c_e$  from now on. This is just the random thermal flux of the electrons reduced by the Boltzmann factor. The total current reaching the probe in this region will be made up of ions and electrons. At  $V_B = V_F$  the net current to the probe is zero,  $I^+ = I^-$ . By equating equation (21) and equation (22) a value for the floating potential is found

$$V_f = V_p - \frac{kT_e}{2e} \ln \left[ \left( 2\pi \frac{m_e}{m_i} \right) \left( 1 + \frac{T_i}{T_e} \right) \right] \quad (23)$$

In a pure hydrogenic plasma  $V_f$  is typically found to be  $\approx -3T_e$  V relative to the plasma potential. As the probe bias continues to rise it will eventually be equal to the plasma potential. At this point there is no potential difference between the probe and the plasma, therefore there are no electric fields and so the sheath disappears. The charged particles now reach the surface of the probe due to their thermal motion and so the probe collects the thermal flux of both electrons and ions. No electrons are repelled any more. Increasing the potential of the probe will act to repel the ions and a negative sheath of electrons now forms around the positive probe to shield out the positive charge. This sheath is very thin and the electric field outside of it is again zero. If the probe bias is sufficiently positive, no ions can reach the probe and the probe collects the electron saturation current. This is just the random thermal flux of electrons that enter the sheath

$$I_{sat}^- = \frac{1}{4} n_0 e c_e A \quad (24)$$

For a pure hydrogenic plasma, with no magnetic fields, the ratio of the electron saturation current to ion saturation current is given by

$$\frac{I_{sat}^-}{I_{sat}^+} \approx 60 \quad (25)$$

Therefore, at bias voltages where  $V_B > V_p$ , the ion contribution to the total current is negligible. For this reason Langmuir probe measurements cannot be used to determine the ion temperature.

Once the probe has been swept an I-V curve can be constructed. In the transition region, the electron current contribution ( $I^-$ ) can be obtained by deducting the ion saturation current from the total current. By rearranging equation 22 it can be seen that

$$\ln(I^-) = \ln(I_{sat}^-) + \frac{e(V_B - V_p)}{kT_e} \quad (26)$$

The electron temperature can then be obtained by plotting  $\ln(I^-)$  against  $V_B$ , the inverse of the gradient giving  $T_e$  in eV. Once  $T_e$  is known, the plasma density can be extracted from the measurement of the ion saturation current, using equation 21. This does require a measurement of  $T_i$ , which is not possible to measure using a standard Langmuir probe. Often the assumption of  $T_i = T_e$  is used, the validity of this assumption is assessed in section 7. As well as Retarding Field Energy analysers discussed in section 7, other advanced probe techniques have been developed to measure  $T_i$ , these are discussed in section 8. Floating potential measurements can be made directly by not biasing the probe or can be inferred from the IV curve as shown in figure 2. In theory the plasma potential can also be read from the IV curve, characterised by the sharp knee. However, in practise, the knee is rounded and so equation 23 is used to determine  $V_p$ . The above equations have all assumed the simplest case of a collisionless sheath with no magnetic field present. All plasma-surface interactions have been neglected. IV curves obtained in tokamak plasmas differ from figure 2 because these assumptions are not always valid. The magnetic field has a strong influence on the dynamics of charged particles and hence the collection of those particles by the probe. The effects of a magnetic field on probe interpretation is discussed in section 5.

## 4 The Pre-sheath in Magnetised Plasmas

For an unmagnetised plasma, the boundary layer between the plasma and a contacting surface consists of a quasi-neutral pre-sheath, which acts to accelerate ions up to the Bohm speed, and the Debye sheath where quasi-neutrality no longer holds. Often in experimental plasmas, such as tokamak experiments, a magnetic field is applied to the plasma to aid in confinement. The presence of the magnetic field affects particle dynamics and changes the constitution of the boundary layer. A numerical model was developed by Chodura [11] to study the effect of an oblique magnetic field, where the angle ( $\alpha$ ) between the field and the tangent to the surface satisfies  $\alpha \neq 90^\circ$ . It was found that there exists three distinct regions between the bulk plasma and the material surface as shown in figure 3. The first region is the familiar pre-sheath which extends far into the plasma. The second region is the Magnetic Pre-Sheath (MPS) which is also quasi-neutral. The size of the MPS scales with the ion Larmor radius and is influenced by the angle between the magnetic field and the surface normal. There is no MPS at normal incidence. The final layer is the familiar electrostatic Debye sheath where quasi-neutrality breaks down.

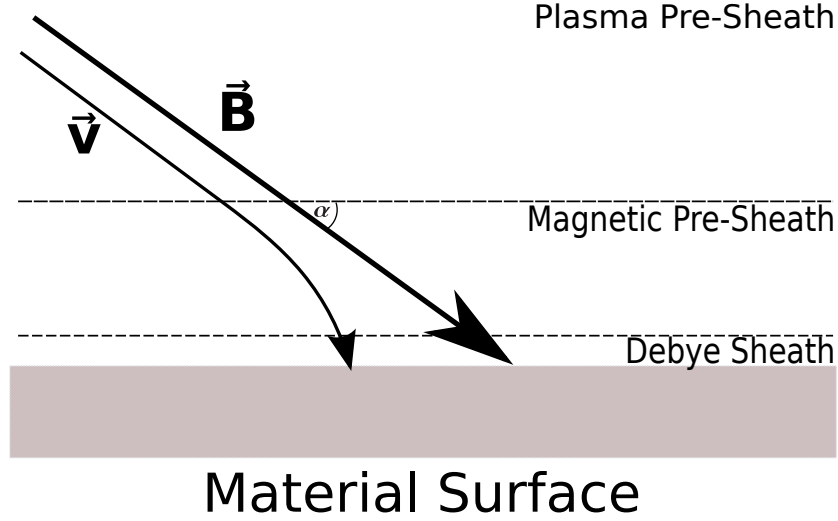


Figure 3: The structure of the sheath in front of a material surface in a magnetised plasma. Particles enter the magnetic pre-sheath with parallel velocity exceeding the Bohm velocity. In the magnetic pre-sheath the particles velocity is turned so that it is sonic perpendicular to the surface on entrance to the Debye sheath.

Chodura found that the role of the pre-sheath in a magnetised plasma is to accelerate ions such that their parallel velocity along the field lines ( $v_{\parallel}$ ) exceeds the Bohm speed on entering the MPS. This is known as the Bohm-Chodura criterion

$$v_{\parallel} \geq c_s \quad (27)$$

Chodura also discovered that the ions velocity was turned from being sonic parallel to the field lines on exiting the pre-sheath to being sonic normal to the surface at the Debye sheath entrance. The role of the MPS is to turn the flow of ions so that they satisfy the Bohm Criterion on entrance to the Debye sheath. The mechanism for this depends on the presence of an electric field in the MPS, the gradient of which results in a polarisation drift [12]. A potential drop ( $V_{MPS}$ ) across the MPS region is responsible for the electric field. The magnitude of this potential drop depends on the angle of attack [13]

$$V_{MPS} = -\frac{kTe}{e} \ln(\sin \alpha) \quad (28)$$

The total potential drop ( $V_f$ ) between the plasma and wall, however, does not depend on the presence of the magnetic field and so the floating potential

of an object in a magnetised plasma is still given by equation 23. The total potential drop is the sum of the potential drop across the MPS and the potential drop across the Debye sheath ( $V_{DS}$ )

$$V_f = V_{MPS} + V_{DS} \quad (29)$$

It was realised by Stangeby [13] that for increasingly lower values of  $\alpha$ , the potential drop across the MPS grows until a critical angle is reached ( $\alpha_c$ ), at which point  $V_{MPS} = V_f$ . For a deuterium plasma, with  $T_e = T_i$ ,  $V_f = 2.84$ . The MPS potential drop will become equal to this once  $\alpha \leq \alpha_c = 3.35^\circ$ . The potential drop in the MPS represents the change in potential required to turn the ion flow from being sonic parallel to the field lines, to sonic normal to the surface. For small  $\alpha$ , there is not enough potential drop across the MPS available to turn the ions towards the surface, the ions therefore exit the MPS with a subsonic velocity normal to the surface. This regime is relevant to fusion devices, with angles of incidence as low as  $1^\circ$  reported in C-mod [14]. Stangeby hypothesised the disappearance of the Debye sheath for angles of incidence below the critical angle. This hypothesis was confirmed by kinetic simulations [15]. For these angles, the electron current to the wall is limited by the magnetic field, with electrons tied to the field lines, whilst the larger ion Larmor radius allows ions to reach the wall more readily. An ambipolar flow to the wall can be maintained without the need for a strong ion acceleration and so the Debye sheath is unnecessary. In extreme cases where  $\alpha < \left(\frac{m_e}{m_i}\right)^{0.5}$ , the larger orbit of the ions means they are the more mobile species, reaching the wall faster and causing it to charge up positively. A more complex sheath arises in this case. The angle at which this would occur in a deuterium plasma is  $\approx \alpha < 1^\circ$ . This regime is currently not applicable to fusion devices as it requires an extremely high degree of alignment of the divertor tiles but it may become relevant with future devices that strive to reduce  $\alpha$  in order to minimise heat and particle flux density to the divertor.

## 5 Probes in Magnetised Plasma

Fusion devices such as tokamaks use strong magnetic fields to confine the plasma long enough for fusion to occur. The presence of a magnetic field changes the dynamics of particles moving in the sheath and so has an impact

on measurements made by probes. Probes are used at the edge of tokamaks to diagnose the plasma at the plasma-surface interface. It is important that the effects of magnetic fields on probe readings are understood in order to correctly interpret probe data. The magnetic field restricts the motion of charged particles. They are free to stream along the field lines (parallel to  $B$ ) but their cross-field motion is now restricted. Charged particles orbit the magnetic field lines in circular orbits with radius equivalent to the Larmor radius ( $\rho_L$ ) given by

$$\rho_L = \frac{vm}{eB} \quad (30)$$

Where  $v$  is the velocity of the charged particle,  $m$  its mass and  $B$  the strength of the magnetic field in Tesla. In an unmagnetised plasma, the dynamics of charged particles are determined by the electric field of the plasma sheath and pre-sheath but with a magnetic field particles can no longer free stream to the probe. The situation is now two dimensional as particles are restricted to following the magnetic field lines. Particle transport to the probe is now restricted by cross-field diffusion and the size of the probe starts to become important. The extent of how probe measurements are affected by the addition of a magnetic field depends on the relative size of the probe dimension  $d$  to that of the Larmor radius. Due to their lower mass the electrons have a much smaller Larmor radius than the ions and so are affected more by the presence of a magnetic field. The probe is described to be in the weak field regime when  $B$  is low enough such that

$$\rho_{L,ion} > \rho_{L,electron} > d \quad (31)$$

In this regime particles are still able to intercept the probe as they orbit the field lines and so particle collection is unaffected. The field free results from ideal theory as previously discussed should still apply. As the strength of the field is increased the Larmor radius decreases. Eventually the dimensions of the probe exceed the Larmor radius of the electrons such that

$$\rho_{L,ion} > d > \rho_{L,electron} \quad (32)$$

this is known as the strong field regime. The ions with their larger mass are relatively unaffected by the magnetic field in this regime, on the other hand the collection of electrons to the probe is restricted as electrons are constrained to orbit the field lines. Electrons will only be collected by the probe if their field line ends on the probe itself, so flow to the probe is

dominated by cross-field transport processes which allow charged particles to move from one field line to another. The flux of particles exiting the flux tube connected to the probe must be balanced by a flux of particles entering the flux tube via cross-field diffusion. It takes a long length of flux tube to balance the two fluxes because parallel transport along the field line occurs much faster than perpendicular transport. This length over which the fluxes become balanced is known as the probe collection length  $L_{col}$  and is illustrated below.

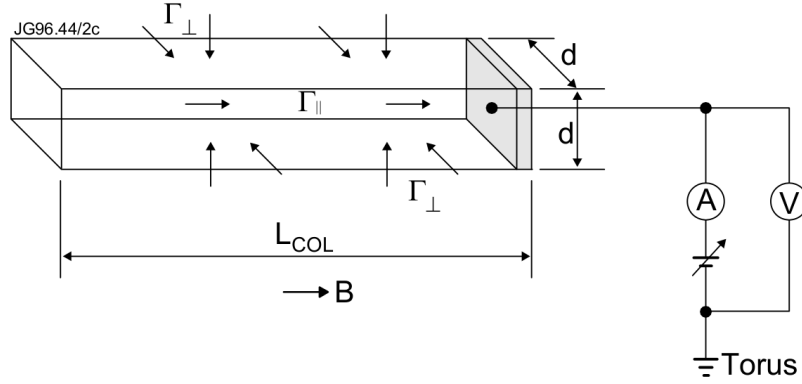


Figure 4: The probe of dimension  $d$  has a collection length associated with it ( $L_{col}$ ) where  $L_{col} \gg d$  [16]

$L_{col}$  is a measure of the distance in which a probe disturbs the plasma it is in. During net electron collection the current drawn by the probe is higher, therefore the collection length increases to balance the higher parallel flux. One consequence of the probe collection length is that measurements from the probe are no longer localised but are averaged over the entire collection length. Electron collection is no longer well described by the random electron flux equation (24) in a magnetised plasma. The most striking evidence that magnetic fields affect probe readings is from observing a dramatic reduction in the electron saturation current to ion saturation current ratio. Bohm predicted values as low as 10 [17] and this was confirmed experimentally by Sugawara [10]. Values for this ratio have been recorded in tokamaks to be even as low as unity [1]. IS THIS BECAUSE THE ELECTRONS ARE MAGNETISED BUT IONS NOT SO ELECTRONS ONLY SEE THE PROJECTED AREA, IONS SEE WHOLE AREA? In JET it was demonstrated that artificially high values of  $T_e$  were obtained when fitting an exponential

to regions of the IV curve where  $V_B > V_F$  [18]. However no significant change in  $T_e$  was observed when using regions below the floating potential. It is now standard procedure to only fit the exponential to regions below the floating potential for probes in magnetised plasma. The more points that are used in the temperature fit from bias voltages greater than the  $V_f$ , the higher the measured temperature [1]. The reason for this is attributed to collisions that occur between the electrons and ions along the collection tube. Regions of increased potential (potential hills) are required, both cross-field and parallel to the field, to attract electrons to the probe. As a result, ions in the probe flux tube find themselves in a retarding field and so obey the Boltzmann relation such that  $n_i \propto \exp(-V/T_i)$ . Therefore a density depression exists just in front of the probe. The electron current to the probe is proportional to the plasma density in front of the probe. A reduced plasma density results in a reduced electron current as compared to the unmagnetised case. The collisions between the ions and electrons constitutes a resistance in what is known as the probe circuit shown in figure 5.

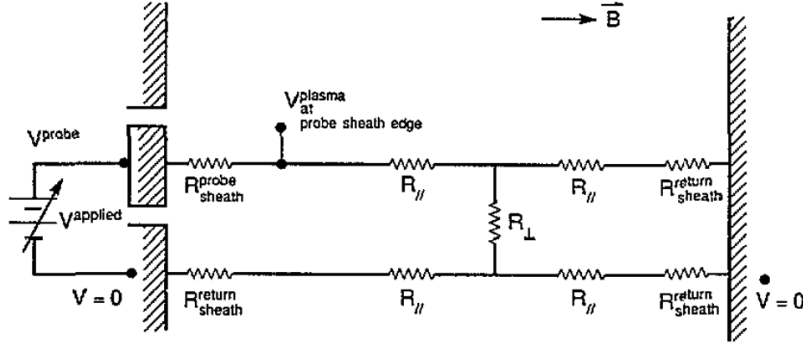


Figure 5: There are various resistances associated with the probe circuit.[19]

In an unmagnetised plasma the only source of resistance is the sheath resistance  $R_{sheath}^{probe}$  and the return sheath resistance  $R_{sheath}^{return}$ . The return sheath completes the probe circuit and is located in between the plasma and the material wall bounding the plasma. The return sheath is present in any probe circuit. Single probe theory is a good approximation in the unmagnetised case provided that the collection area of the return sheath is much greater than the collection area of the probe sheath. If this is true it can be assumed that  $R_{sheath}^{return} = 0$  as resistance is inversely proportional to area. In the case when  $B = 0$  the area of the return sheath is essentially the surface area of



the vessel wall and so this requirement is met. No other sources of resistance are present so the probe bias only appears across the probe sheath. If this is the case then the IV characteristic is defined by

$$I = I_{sat}^+ \left[ 1 - \exp\left(\frac{(V - V_F)}{kT_e}\right) \right] \quad (33)$$

where  $V$  is the value of the voltage drop across the sheath.  $V = V_B - V_s$  with  $V_B$  being the applied probe voltage and  $V_s$  the plasma potential at the sheath edge of the probe. With no other sources of resistance present, the entirety of the applied voltage to the probe is contained in the sheath and so  $V_s = 0$ . Adding a magnetic field introduces new sources of resistance including the parallel resistance  $R_{\parallel}$  and perpendicular resistance  $R_{\perp}$ . The applied voltage to the probe is now shared between the probes sheath resistance and all other sources of resistance in the circuit and because of this it is no longer valid to assume  $V_s = 0$ . Without knowing the value for  $V_s$  it is not possible to use (33) to derive  $T_e$ . In principle it could be possible to model all the other sources of resistance within the circuit in order to calculate the probe-sheath resistance which would then give  $V_s$  but cross-field transport mechanisms are not well understood.

$R_{\perp}$  is the resistance associated with cross field transport and could have different values for ions and electrons. It can not be modelled due to the lack of understanding of cross-field transport mechanisms.  $R_{\parallel}$  is the resistance associated with parallel transport. Sources include friction caused by collisions with neutral particles and friction between the oppositely charged electrons and ions. The inability to model perpendicular resistance also prevents us from modelling the two other resistances in the circuit.  $R_{sheath}^{return}$  depends on the area of the return sheath which in turn depends on the ratio of parallel to perpendicular transport. This ratio also determines whether or not the probe circuit extends to the other divertor target or closes back on itself. The path it takes will impact the parallel resistance. Because these resistances cannot be modelled it is not possible to calculate the value of  $V_s$  unless  $R_{sheath}^{probe} \gg R$  where  $R$  is all other forms of resistance in the circuit. If this is the case, single probe theory can be used to extract  $T_e$  when the plasma is magnetised.

Naturally the question arises - can Langmuir probes be used reliably in magnetised plasmas? Experiments with a pin-plate probe were conducted to test if the portion of the IV curve below floating could be used safely to derive  $T_e$  [20]. The pin-plate probe consisted of a Langmuir probe plate, with dimensions 10 mm x 5 mm and a pin probe of diameter 1 mm and a length of

5 mm, placed 2.5 mm in front of the plate. The pin was operated in floating mode for the duration of the experiment whilst the plate probe was swept as with a standard Langmuir probe. A schematic of the pin-plate probe is shown in figure 6. The floating potential of the pin was representative of the plasma potential outside the plate sheath, offset by a factor assumed to be constant. The experiments found that the potential on the floating pin remained almost constant for bias voltages on the plate that satisfied  $V_B^{plate} < V_F^{plate}$ . It can be concluded from this that for these bias voltages, the plate potential was entirely contained in the plate sheath and so  $R_{sheath}^{probe} \gg R$ . As a result  $T_e$  can be extracted safely from this region. There was a slight increase of a few volts once  $V_B$  was within a few  $T_e$  of floating i.e.  $V_F - 3T_e \leq V_B \leq V_F$ . This was attributed to either an extraneous effect or some of the probe bias appearing elsewhere in the probe circuit. If the later were true, the paper expects between a 15%  $\rightarrow$  20% error in the  $T_e$  measurement when using this region. For bias voltages such that  $V_B^{plate} > V_F^{plate}$  it was found that the pin floating potential increased monotonically with the bias voltage applied to the plate. This is due to the formation of a potential hill which is established to drive the electron current to the probe against the friction of the ions in the probe collection tube. This potential hill results in a reduced plasma density in front of the probe which leads to a reduced electron current. The electron current in this region no longer behaves as a simple exponential. Including points from this region in the exponential fit will result in a spuriously high measurement of the electron temperature. In later work, Stangeby concluded that it is a reasonable assumption to use the region of the IV curve below floating potential to yield a reliable value of  $T_e$  [21].

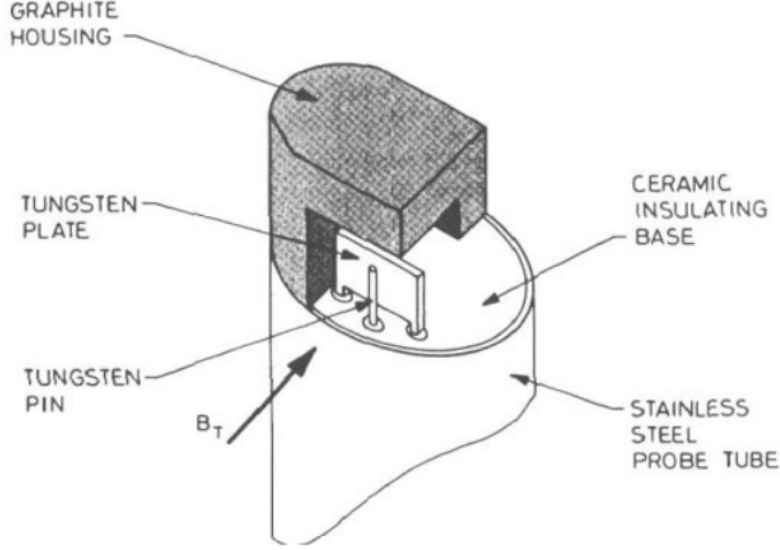


Figure 6: The pin-plate probe consisting of a tungsten pin located in front of a tungsten plate. [21].

Once a probe is operating in the strong regime, the effects of the magnetic field must be taken into account in order to reliably measure the electron temperature. Increasing the field further leads to the 'very strong field' regime. This is defined at the point where

$$d > \rho_{L,ion} > \rho_{L,electron} \quad (34)$$

The motion of both electrons and ions is now strongly affected by the field. It is simple to see whether or not this regime is relevant to fusion. As a typical example the field in the divertor region of JET is  $\approx 3T$  and the electrons and ions have a temperature of around  $10eV$ . This gives the ions a Larmor radius of  $\approx 0.1mm$  while probes are typically  $2mm$  long. The high temperatures in this region place a constraint on the size of the probes as they need to be large enough to dissipate the heat and avoid being melted, so making the probes smaller in order to simplify probe interpretation is not a viable option. In this regime, particles are only able to reach the probe from the direction parallel to the field so it appears to them that the probe has a plane geometry regardless of its actual geometry. This means the effective collection area of the probe ( $A_{eff}$ ) is now reduced from its actual surface area ( $A_{surface}$ ) to the

projection of the surface ( $A_{proj}$ ) in the direction of the field

$$A_{eff} = A_{proj} = A_{surface} \sin(\theta) \quad (35)$$

where  $\theta$  is the angle between the field and probe as shown in figure 7. The shape of the probe in this regime is not very important only its cross sectional area perpendicular to  $\vec{B}$  [19]. As demonstrated by equation 21, the effective collection area of the probe must be known in order to determine the plasma density from measurements of the ion saturation current. Experiments were carried out by Brown in a linear plasma device that contained two sets of diagnostics capable of measuring the electron density, Langmuir probes and a microwave interferometer [22]. Both diagnostics were used simultaneously whilst the magnetic field strength was increased. As the field became stronger, the electron density derived from probe readings deviated from those obtained by the interferometry. The probes gave a lower value of  $n_e$  than measured by the interferometry. This can be explained by a reduction in the collection area of the probe due to the increased field which then results in a lower value for  $I_{sat}^+$ . If the effects of the magnetic field are not taken into account the plasma density will be underestimated and the electron temperature overestimated.

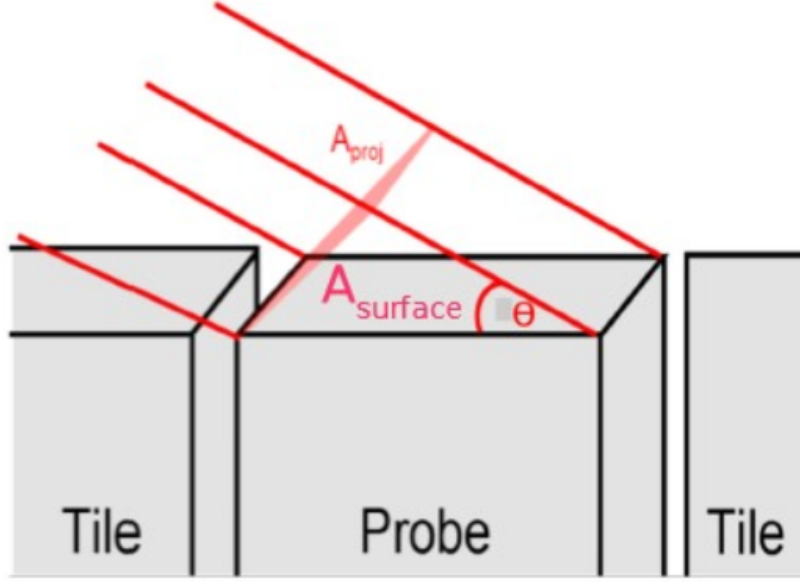


Figure 7: In a strongly magnetised plasma the effective collection area of the probe is reduced from its surface area ( $A_{surface}$ ) to the projection of that surface perpendicular to the magnetic field ( $A_{proj}$ ).

## 6 Langmuir Probes in Tokamaks

A tokamak plasma with high temperature and density is a hostile environment for a material surface. Any material placed into the plasma, such as a probe, will suffer damage from the high heat and particle flux impinging on it. This is also true of probes placed in the relatively cooler and less dense SOL region. Steps have to be taken to ensure the probes survive the plasma conditions so that useful measurements can be taken. It is also important that the probe does not contaminate the plasma, particularly with high  $Z$  impurities which reduce the temperature of the plasma by radiative cooling. Various techniques have been developed to enhance the lifetime of tokamak probes. One technique is to place the probes in a reciprocating probe head. This head can be submersed into the SOL via a drive mechanism which is connected to a support structure. The drive mechanism plunges the head into a region of the SOL, the probe then takes its measurements before being retracted back into the vacuum region away from the plasma. An additional

benefit of reciprocating system is that it allows the probe to measure different depths of the SOL plasma, allowing SOL profiles to be constructed. The probe head may be exposed to plasma for  $\approx 100$  ms during a typical plunge. It is advantageous for the probe head to be as light as possible so that it can be quickly accelerated into and out of the plasma. It must also be able to survive heat fluxes on the order of  $10 \text{ MW/m}^2$  [2]. Graphite is the material of choice in many tokamaks as it is a low Z material capable of withstanding the hostile conditions presented by the plasma. Low Z impurities result in less cooling to the core due to radiative cooling. However, over time, damage to the probe is inevitable. Modular designs are often employed on modern tokamaks to aid in the task of probe replacement. Another technique is to use heat sink probes that are in good thermal contact with a large heat sink.

An alternative probe design is to align the probe so that its surface is flush with the surrounding divertor tiles. These Flush Mounted Probes (FMP) are one of the most robust probe designs and they are almost as resilient as the divertor tiles, sharing the same geometry relative to the magnetic field [23]. The grazing angle between the field and the FMP in the divertor region means the intense heat flux is spread out over a larger area thus reducing the damage to the probe. This grazing field line can lead to complications in interpreting the data obtained from FMPs as the projected area of the probe can become comparable to the sheath area for such small field line angles. This will be discussed further in Chapter X.

## 7 Underlying Assumptions of Probe Theory

In deriving the equations of section 3 it was assumed the particles had a Maxwellian velocity distribution. A reciprocating probe was used on COM-PASS to evaluate the velocity distribution of electrons within the last closed flux surface (LCFS) and the SOL. Within the LCFS and SOL, evidence for a bi-Maxwellian distribution of electrons was found, corresponding to two Maxwellian distributions of electrons at different temperatures [24]. This has also been reported on CASTOR [25] and NSTX [26]. This can lead to errors in the electron temperature measurement, especially if the I-V curve is only swept up to the floating potential, in which case only the high energy tail of the electron distribution is sampled. In the far SOL, close to the walls it was found that the electrons adopted a single Maxwellian distribution and so the assumption was valid in this region of the tokamak. A value for  $T_i$  is

required to obtain the plasma density from the ion saturation current. Due to difficulties in obtaining a measurement for this value it is often assumed to be the same as the measured  $T_e$  value. Retarding Field Energy Analysers (RFEA) can be used to obtain measurements of  $T_i$ , by using a series of charged plates and grids to repel electrons and only collect the ions. The exponential drop off of the ion current, as the bias voltage is swept, can then be used to extract  $T_i$ . Two RFEAs were placed on MAST to measure the ion temperature [27]. It was found that for low power L-mode plasma discharges,  $T_i = T_e$  was a good assumption at the target and in the SOL. However, for higher power discharges and in H-mode, ratios of  $T_i/T_e = 1 \rightarrow 3$  were observed so this assumption may not always hold.

## 8 Advanced Probe Designs

A whole range of advanced probe techniques have been developed in order to measure quantities such as the plasma potential, electron temperature, electron density and ion temperature without the limitations of standard Langmuir probes discussed above. Ball-pen probes and emissive probes aim to measure the plasma potential directly by reducing the ratio of the saturation currents to one such that the probe floats at the plasma potential [28]. These will be discussed in Chapters X and Y respectively. BPP's and LP's can be used simultaneously to provide fast measurements of  $T_e$ , this will also be discussed in Chapter X. A segmented tunnel probe has been developed that is capable of measuring the electron temperature without actually collecting any electrons [29]. The probe is U-shaped, consisting of a conducting tunnel and a conducting backplate. Both conductors are biased sufficiently negatively to repel all electrons. The ion current collected by each conductor is measured. The ratio of the currents to each collector depends on the thickness of the sheath at the entrance to the tunnel which in turn depends on  $T_e$ . This relationship is derived from Particle-In-Cell modelling of the probe. By adding a conducting diaphragm around the entrance to the tunnel it is possible to prevent electrons from reaching one of the tunnel segments [30]. By sweeping the bias voltage across this segment, an exponential fall off in the ion current is observed. This data is hidden by the electron current for a standard probe. The rate at which the ion current decreases allows  $T_i$  measurements to be made. The segmented tunnel probe is one example of a family of probes that aim to shield the electrons from a collector so that the

ion current can be analysed. These Ion Sensitive Probes (ISP) often exploit the difference in Larmor radii of the electrons and ions to inhibit electrons from reaching a part of the probe [31].

## 9 Summary

Sheath theory has been introduced as this underpins measurements made by electric probes in plasmas. Standard Langmuir probe theory has been introduced and complications in probe interpretation arising from the presence of magnetic fields have been discussed, this will be explored further in chapter X. Various advanced probe techniques have been summarised, of these the BPP and emissive probe will be studied in chapter Y and Z respectively.

## 10 References

### References

- [1] G F Matthews. Tokamak plasma diagnosis by electrical probes. *Plasma Physics and Controlled Fusion*, 36(10):1595, 1994.
- [2] J. A. Boedo M. Groth N. H. Brooks A. McLean B. LaBombard C. H. Skinner D. L. Rudakov W. P. West C. P. C. Wong C. J. Lasnier, S. L. Allen. Chapter 10: First wall and operational diagnostics. *Fusion Science and Technology*, 53(2):640, 2008.
- [3] H. M. Mott-Smith and Irving Langmuir. The theory of collectors in gaseous discharges. *Phys. Rev.*, 28:727–763, Oct 1926.
- [4] Evgeny V. Shun’ko. *Langmuir Probe in Theory and Practise*. Universal Publishers, 1 edition, 2009.
- [5] K-U Riemann. The bohm criterion and sheath formation. *J.Phys.D:Appl.Phys.*
- [6] P C Stangeby. A tutorial on some basic aspects of divertor physics. *Plasma Physics and Controlled Fusion*, 42(12B):B271, 2000.
- [7] D Bohm. The characteristics of electrical discharges in magnetic fields. *A Guthry and R K Wakerling ch 3, pg 77*.



- [8] P C Stangeby. *The Plasma Boundary of Magnetic Fusion Devices*. IoP, 2000.
- [9] Robert B. Lobbia and Alec D. Gallimore. Temporal limits of a rapidly swept langmuir probe. *Physics of Plasmas*, 17(7), 2010.
- [10] Raymond David Monk. Langmuir probe measurements in the divertor plasma of the jet tokamak. 1996.
- [11] R. Chodura. Plasmawall transition in an oblique magnetic field. *Physics of Fluids*, 25(9), 1982.
- [12] Spilios Riyopoulos. Unstable particle drift across a magnetic field caused by oblique electric field gradients. *Physics of Plasmas*, 3(12), 1996.
- [13] P.C. Stangeby. The chodura sheath for angles of a few degrees between the magnetic field and the surface of divertor targets and limiters. *Nuclear Fusion*, 52(8):083012, 2012.
- [14] A.Q. Kuang, D. Brunner, B. LaBombard, R. Leccacorvi, and R. Vieira. Design and operation of a high-heat flux, flush-mounted rail langmuir probe array on alcator c-mod. *Nuclear Materials and Energy*, pages –, 2016.
- [15] David Coulette and Giovanni Manfredi. Kinetic simulations of the chodura and debye sheaths for magnetic fields with grazing incidence. *Plasma Physics and Controlled Fusion*, 58(2):025008, 2016.
- [16] P C Stangeby. Effect of bias on trapping probes and bolometers for tokamak edge diagnosis. *Journal of Physics D: Applied Physics*, 15(6):1007, 1982.
- [17] McGraw-Hill. The characteristics of electrical discharges in magnetic fields. *National nuclear energy series*, 5, 1949.
- [18] J A Tagle, P C Stangeby, and S K Erents. Errors in measuring electron temperatures using a single langmuir probe in a magnetic field. *Plasma Physics and Controlled Fusion*, 29(3):297, 1987.
- [19] P C Stangeby. Determination of  $t_e$  from a langmuir probe in a magnetic field by directly measuring the probe’s sheath drop using a pin-plate probe. *Plasma Physics and Controlled Fusion*, 37(11):1337, 1995.

- [20] R A Pitts and P C Stangeby. Experimental tests of langmuir probe theory for strong magnetic fields. *Plasma Physics and Controlled Fusion*, 32(13):1237, 1990.
- [21] P C Stangeby. Determination of  $t_e$  from a langmuir probe in a magnetic field by directly measuring the probe's sheath drop using a pin-plate probe. *Plasma Physics and Controlled Fusion*, 37(11):1337, 1995.
- [22] Ian G. Brown, Alan B. Compher, and Wulf B. Kunkel. Response of a langmuir probe in a strong magnetic field. *Physics of Fluids (1958-1988)*, 14(7), 1971.
- [23] A. Carlson, V. Rohde, and M. Weinlich. The separation of angle and size effects on langmuir characteristics. *Journal of Nuclear Materials*, 241:722 – 727, 1997.
- [24] M Dimitrova, Tsv K Popov, P Ivanova, E Vasileva, E Hasan, J Horek, P Vondrek, R Dejarnac, J Stckel, V Weinzettl, J Havlicek, F Janky, and R Panek. Evaluation of the scrape-off-layer plasma parameters by a horizontal reciprocating langmuir probe in the compass tokamak. *Journal of Physics: Conference Series*, 514(1):012049, 2014.
- [25] Tsv K Popov, P Ivanova, J Stckel, and R Dejarnac. Electron energy distribution function, plasma potential and electron density measured by langmuir probe in tokamak edge plasma. *Plasma Physics and Controlled Fusion*, 51(6):065014, 2009.
- [26] M.A. Jaworski, M.G. Bell, T.K. Gray, R. Kaita, J. Kallman, H.W. Kugel, B. LeBlanc, A.G. McLean, S.A. Sabbagh, V.A. Soukhanovskii, D.P. Stotler, and V. Surla. Modification of the electron energy distribution function during lithium experiments on the national spherical torus experiment. *Fusion Engineering and Design*, 87(10):1711 – 1718, 2012. The 2nd International Symposium of Lithium Application for Fusion Devices.
- [27] S Elmore, SY Allan, A Kirk, AJ Thornton, JR Harrison, P Tamain, M Kočan, JW Bradley, MAST Team, et al. Scrape-off layer ion temperature measurements at the divertor target in mast by retarding field energy analyser. *Journal of Nuclear Materials*, 438:S1212–S1215, 2013.

- [28] G Van Oost. Advanced probe edge diagnostics for fusion devices. *Journal of Physics: Conference Series*, 666(1):012001, 2016.
- [29] J. P. Gunn, R. Schrittwieser, P. Balan, C. Ioni, J. Stckel, J. Admek, I. uran, M. Hron, R. Pnek, O. Baina, R. Hrach, M. Vicher, G. Van Oost, T. Van Rompuy, and E. Martines. Tunnel probes for measurements of the electron and ion temperature in fusion plasmas. *Review of Scientific Instruments*, 75(10):4328–4330, 2004.
- [30] P. Balan, R. Schrittwieser, J. Admek, O. Baina, P. De Beule, I. uran, J. P. Gunn, R. Hrach, M. Hron, C. Ioni, E. Martines, R. Pnek, J. Stckel, G. Van Den Berge, G. Van Oost, T. Van Rompuy, and M. Vicher. Measurements of the parallel and perpendicular ion temperatures by means of an ion-sensitive segmented tunnel probe. *Contributions to Plasma Physics*, 44(7-8):683–688, 2004.
- [31] I. Katsumata. A review of ion sensitive probes. *Contributions to Plasma Physics*, 36(S1):73–79, 1996.